Attaining both Coverage and High Spectral Efficiency with Adaptive OFDM Downlinks

Mikael Sternad[*], Tony Ottosson[†], Anders Ahlén[*], and Arne Svensson[†]

[*]Signals and Systems, Uppsala University, PO Box 528, SE-751 20 Uppsala, Sweden

[†]Dept. of Signals and Systems, Chalmers University of Technology, SE-41296 Göteborg, Sweden

{mikael.sternad, anders.ahlen}@signal.uu.se; {tony.ottosson, arne.svensson}@s2.chalmers.se

Abstract— **A downlink radio interface is proposed for cellular packet data systems with wide area coverage and high spectral efficiency. A slotted OFDM radio interface is used, in which time-frequency bins are allocated adaptively to different users within a downlink beam, based on their channel quality. Fading channels generated by vehicular 100 km/h users may be accommodated. Frequency division duplex (FDD) is assumed, which requires channel prediction in the terminals and feedback of that information to a packet scheduler at the base station. To attain both high spectral efficiency and good coverage within sectors/beams, a scheme based on coordinated scheduling between sectors of the same site, and the employment of frequency reuse factor above 1 only in outer parts of the sector, is proposed and evaluated. The resulting sector throughput increases with the number of active users. When terminals have one antenna and channels are Rayleigh fading, it results in a sector payload capacity between 1.2 (one user) and 2.1 bits/s/Hz/sector (for 30 users) in an interference-limited environment.**

I. INTRODUCTION

The successful deployment of OFDM in several standards and demonstrators has increased the interest in applying it also in new broadband air interfaces beyond 3G [1]. OFDM is inherently scalable to higher bandwidths, it is spectrally efficient and it avoids the intra-cell interference problems of CDMA systems. Spectral efficiency and peak data rates may be increased further by deploying adaptive OFDM multiplexing. Multiple users then share the available bandwidth, and resources are allocated to the terminals who at the moment need them best and/or can utilize them best via link adaptation. The resulting spectral efficiency will increase with the number of active users, an effect sometimes denoted multiuser diversity. A key issue in this context is to find appropriate scheduling strategies for different service classes [2].

The present paper outlines the downlink of an adaptive OFDM system that employs FDD. A base station infrastructure is assumed and the aim is a design that is feasible also for vehicular users, around 100 km/h.[1] The proposed downlink is specified in Section II and Section III below. The quality of downlink channels must in such a solution be predicted by the terminals, and reported to the base stations. The corresponding multiuser diversity effect and the required control bandwidth is investigated in [4].

High data rates and high spectral efficiency due to low interference can be attained if coverage is sacrificed, as in the

Infostation proposal of [5]. In a system with wide area coverage, interference from other cells will be a major problem, and will limit the modulation formats and data rates that can be utilized. The interference problem can be reduced by cell planning with a high frequency reuse factor, but this would reduce the overall spectral efficiency. Can the proposed radio interface be deployed with wide area coverage and still retain high spectral efficiency? A solution to this problem, based on coordinated scheduling between sectors of the same site, and the employment of frequency reuse > 1 only in outer parts of the sectors, is outlined in Section IV. A preliminary evaluation is presented in Section V for an interference-limited scenario with 60 degree sectors in a hexagonal site pattern. It indicates that e.g. a sector payload capacity of 2 bits/s/Hz/sector will then be attained in our proposed downlink for 5 active users/sector, each having 2 antennas. This value is an average over random locations within the sector, with Rayleigh fading channels. The equivalent reuse factor is below 2.

II. AIMS, TOOLS, AND CONSTRAINTS

The proposed downlink is designed to attain high spectral efficiency for delay-insensitive traffic classes, as well as low link-level retransmission delays. The downlink channel may have delay spreads corresponding to up to 3 km distance, and vehicle speeds may be around 100 km/h. For ease of comparison with WCDMA, the design is exemplified by assuming a 1900 MHz carrier.

A conventional approach to wireless system design uses coding, spreading, interleaving to average out channel variations. That approach may create a reliable channel but it limits the spectral efficiency. The main design principle here is instead to utilize channel state information to adapt the signaling, and use coding only sparingly. Several tools may be used for this purpose:

- Fast link adaptation can adjust the transmission rate to channels that vary in time due to short-term fading [6]. This requires channel prediction and also interference suppression, to enable the use of high data rates [7]. In a wide-band system, the fading will differ at different sub-frequencies. This provides another dimension over which to perform resource allocation/scheduling, and suggests the use of an OFDM transmission scheme.

- Multiple transmit antennas in each sector and multiple antennas at mobile terminals can be used to suppress in-

---

[1]The system serves as a focus for our research within the Wireless IP project [3], supported by the Swedish Foundation for Strategic Research.

terference, increase the transmission range, or to improve the throughput by MIMO spatial multiplexing.

- Channels to different users will fade independently. With many active users, the channel could almost always be allocated to users who encounter favorable conditions. The spectral efficiency will then increase with the number of active users, an effect sometimes denoted multiuser diversity [8]. Its exploitation requires prediction of channel variations. It also requires appropriate scheduling algorithms to distribute resources among users.

We here restrict the attention to downlinks, assuming an uplink of similar capacity and design to be available [9]. The discussion is restricted to a base station infrastructure, with sectored antennas. The sectors or beams constitute cells. They may either be conventional (fixed), or their beamwidths and angles may be slowly adjusted adaptively, based on the traffic requirements. There are K active users within a sector (cell) who have L receiver antenna branches each. Transmitters are in this paper assumed to have only one diversity branch per sector. This case serves as a baseline against which we at present compare various MIMO solutions.

Furthermore, we assume different frequency bands for the uplink and the downlink (FDD). This avoids the severe synchronization problems of time division duplex (TDD) solutions, but requires a considerable amounts of channel state information to be transmitted from mobiles to the scheduler.

We consider the setting with simultaneous wide area coverage, high vehicle speeds and FDD partly because it is difficult. Methods that work well in this situation will probably work also for simpler scenarios.

III. THE PROPOSED ADAPTIVE OFDM DOWNLINK

A. The Physical Layer

The available downlink bandwidth, s, within a sector is assumed to be slotted in time. Each slot of duration T is partitioned into *time-frequency bins* of bandwidth Δf_b. The channel is assumed to be described by a complex scalar, which varies only slightly within a bin. This assumption restricts the bin size. In [4], we discuss the choice $T = 0.667$ ms and $\Delta f_b = 200$ kHz as appropriate for stationary and vehicular users in urban or suburban environments [2]. This size represents a reasonable balance between the spectral efficiency of the downlink and the required uplink control bandwidth.

We also assume a subcarrier spacing of 10 kHz, a cyclic prefix of length 11μs and an OFDM symbol period (including cyclic prefix) of $T_s = 111\mu$s. Thus, each bin of 0.667 ms × 200 kHz carries 120 symbols, with 6 symbols of length 111μs on each of the 10 kHz subcarriers. Of these 120 symbols, 12 are allocated for training and downlink control, leaving 108 payload symbols that constitute the link-level packets. The 12 pilots and control symbols are located within each bin as

---

[2]For example, for Jakes fading with exponential power delay profile $p(\tau) = (1/\sigma)e^{-\tau/\sigma}$, where τ is the delay and σ is the RMS delay spread, the correlation in the frequency domain between the fading of subcarriers at the center of the bin and at the bin boundary (100 kHz difference) will then be high for σ up to 1μs [10].
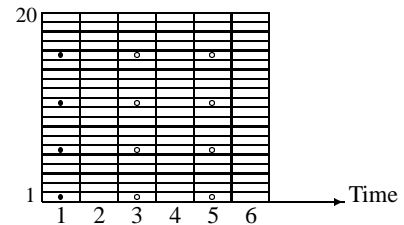

Fig. 1. One of the time-frequency bins of the proposed system, containing 20 subcarriers with 6 symbols each. Known 4-QAM pilot symbols (black) and 4-QAM downlink control symbols (rings) are placed on four pilot subcarriers. The modulation format for the other (payload) symbols is adjusted adaptively. All payload symbols within a bin use the same modulation format.

indicated by Fig. 1. They are assumed to use 4-QAM and can be detected by all users within the sector. They are transmitted in all bins, also bins without payload data.

All active users must estimate the channel within the whole bandwidth. The channel estimates are used for two purposes: In bins addressed to a user, coherent detection of the payload symbols requires the received signal to be divided by the channel estimate. Channel estimates at the pilot locations within all bins are furthermore used as regressors by the predictor, see Subsection C. Novel channel estimation algorithms that are designed for these purposes and that are based on low-complexity approximations of the optimal Kalman state estimator are presented in the companion paper [11].

B. Resource Allocation

During slot j, each terminal predicts the signal to interference and noise ratio (SINR) for all bins, with a prediction horizon mT which is larger than the time delay of the transmission control loop. All terminals then signal their predicted quality estimates on an uplink control channel. They transmit the suggested appropriate modulation formats to be used within all bins of the predicted time slot $j + m$. In our baseline design, we assume an adaptive modulation system that uses 8 uncoded[3] modulation formats: BPSK, 4-QAM, 8-PSK, 16-QAM, 32-QAM 64-QAM, 128-QAM, and 256-QAM. This adaptive modulation system is optimized and evaluated in the companion paper [4]. It is designed to maximize the spectral efficiency for each user for constant transmit power, by balancing the throughput when using 2^{k_i} bits per symbol against the capacity loss due to erroneous packets. The resulting rate boundaries are presented in Table I.

A scheduler that is located at the base station then allocates these time-frequency bins exclusively to different users and broadcasts its allocation decisions.[4]

---

[3]The use of adaptive trellis-coded M-QAM based on the predicted channel quality [12] would improve the performance by attaining the same spectral efficiency as our uncoded baseline scheme at 1-2 dB lower SNR.

[4]A user number per bin is indicated. This information is important, and should be protected by coding. For $K \le 2^n$ simultaneous users and a code rate R, this will require n/R bits/bin. Four of the control symbols (8 bits with QPSK) should be adequate, with, for example, $K \le 32$ users and $R = 5/8$. The downlink also carries uplink control information (decisions on who will use future uplink bins). This requires similar bit-rates as for the downlink broadcast and utilizes the remaining four control symbols.

In addition to the predicted transmission formats, the scheduler should also take the buffer contents and the quality of service requirements (packet error probabilities and delays) for each data stream into account. This is illustrated by Fig. 2.

When the scheduling for slot $j + m$ is complete, bits from appropriate queues are formed into link level packets, modulated with a modulation alphabet appropriate for the predicted channel quality and are then transmitted in their appropriate bins. The modulation formats used in different bins are those which were suggested by the appointed users. A link level packet thus consists of $108 \times k_i$ bits, where k_i is the number of bits per symbol.

A CRC checksum is used to detect erroneously received link-level packets and link-level retransmission is then performed. The maximum number of retransmission attempts depends on the delay sensitivity of the traffic class. The minimum retransmission delay, mT, is short. This reduces undesired effects on TCP flow control mechanisms.

i	Modulation	k_i	γ_i (dB)
0	BPSK	1	$-\infty$
1	4-QAM	2	8.70
2	8-PSK	3	14.58
3	16-QAM	4	16.84
4	32-Cross-QAM	5	20.46
5	64-QAM	6	23.59
6	128-Cross-QAM	7	26.86
7	256-QAM	8	29.94

TABLE I

OPTIMIZED SWITCHING LEVELS γ_i FOR THE LOWEST SINR PER SYMBOL AND RECEIVER ANTENNA FOR USING MODULATION WITH k_i BITS PER SYMBOL. FROM [4].
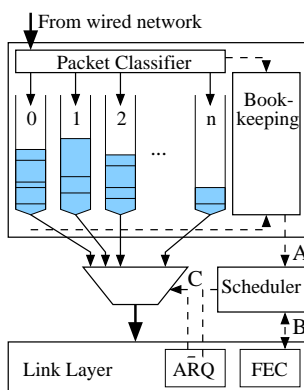

Fig. 2. From [13]. The downlink buffer and the scheduler. Packets arrive at the top and are inserted into their respective queues, restoring order among occasionally arriving out-of-order packets. The buffer regularly submits a status report (A) to the scheduler, containing information about the priorities, the size of the queues, and the required link service. The scheduling decision (C) gives high priority to retransmissions of erroneous packets (link-level ARQ). The queues are drained with a bit-level resolution, to form link level packets that contain $108k_i$ bits, where k_i depends on the user the and bin location.
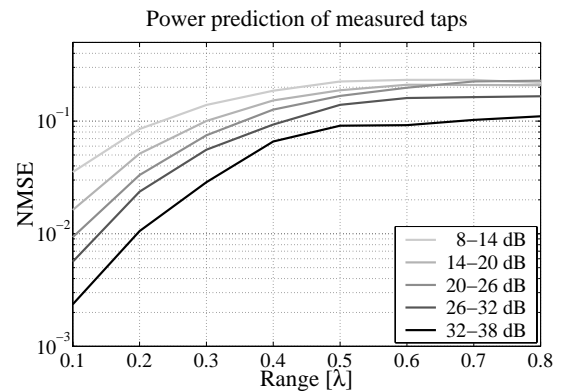

Fig. 3. From [14]. The median of the power prediction normalized mean square error (NMSE) as a function of the prediction horizon in wavelengths, for an unbiased quadratic power predictor based on a least squares-adjusted FIR predictor of complex taps [15]. Smoothed regressors and 8 FIR coefficients are used for predicting one complex tap. The five curves correspond to different SNR's on the complex taps, which correspond to the estimation-error-to noise ratio of the old tap estimates that are used as regressors. The lower the SNR, the higher the NMSE. The results are based on channel sounding measurements at 1880 MHz with 6.4 MHz sampling rate, that were collected at 41 locations, with vehicle velocities from 20 to 90 km/h.

C. Prediction and Feedback Delays

Prediction of the whole channel with horizon mT can be performed either in the time domain or in the frequency domain.[5] Fig. 3 summarizes the attainable measured performance of channel tap power prediction. The best known power prediction performance on measured broadband data is obtained with the unbiased quadratic power predictor presented in [15]. It is evident from Fig. 3 that the prediction accuracy decreases with an increasing prediction horizon. A low error variance in the channel estimates that are used as regressors by the predictor is advantageous. It improves the prediction accuracy.

These results on the predictability provide crucial input to the choice of feedback system in the adaptive OFDM control loop. A reasonable assumption for the total loop delay (prediction time, uplink control signaling and scheduling) is two time-slots $(2T)$. A link-level retransmission could be performed on this timescale, which is very fast compared to typical TCP round trip times. A control loop delay of $2T$ would require a prediction horizon of $m = 3$ or $3T = 2.0$ ms.

Prediction over 2 ms seems attainable at 1900 MHz also for the fastest considered users, at 100 km/h vehicle speed. If, for example, an NMSE of 0.1 is deemed acceptable, this would correspond to 0.34 wavelengths at 100 km/h vehicle speed and 1900 MHz carrier frequency. Fig. 3 indicates that this is attainable at realistic SINR's.

---

[5]The frequency-domain Kalman-based estimators discussed in [11] could be used to also perform prediction of the short-term fading. However, for physical reasons [14], improved accuracy should be obtained by predicting individual channel taps in the time domain. Inverse FFT's are then applied to the frequency domain channel and interference estimates. The resulting sequence of impulse responses is used by time domain predictors that extrapolate the significant impulse response taps and the interference level. An FFT then provides the predicted frequency domain channel, and the SINR.

What effect would a prediction NMSE of 0.1 have on the adaptive modulation? The effect of the prediction error on an adaptive uncoded M-QAM modulation system, and adjustments of the SINR limits for the modulation levels that take the prediction accuracy into account, have been investigated in [7]. Based on these results, a power prediction NMSE of 0.1 reduces the attainable spectral efficiency by around 10% at an average SINR of $\bar{\gamma} = 16$ dB for $L = 1$ and $K = 1$, while a smaller reduction can be expected for a larger number K of simultaneously active users. Thus, a design based on prediction horizons of 2 ms, leading to a prediction error NMSEs of around 0.1, seems reasonable.

The predictors discussed above are designed to predict the short-term (Rayleigh) fading, to provide input to the scheduler. Predictor on longer time-scales could be of interest for predicting the shadow fading (or log-normal fading). Such predictions of the channel state variations over intervals measured in seconds could potentially be of use in the transport layer, in particular for active queue management of the queues in Fig. 2.

IV. RESOURCE PARTITIONING AND SCHEDULING BETWEEN SECTORS

We now consider strategies to reduce the interference level in the system. All sectors at all sites are assumed to use the same bandwidth s. Thus, the basic frequency reuse factor is 1. The following two methods are proposed for attaining coverage within sectors while retaining a high spectral efficiency.

1) Interference from other sites will on average be strongest, and the signal strength weakest, near the outer sector border. Therefore, the sector is divided into an inner zone 1 which is allocated a bandwidth s_1 and an outer zone 2 that uses the remaining bandwidth s_2, where $s_1 + s_2 = s$. The bandwidth s_1 is used at all sites while the bandwidth s_2 is shared among sites in a classical reuse 3 pattern, to reduce interference from neighboring sites in the outer zone 2. The spectral efficiency is thereby reduced by a factor $c_2 = (s_1 + (1/3)s_2)/s$.

2) The scheduling for sectors belonging to the same site is coordinated in the following way: When transmitting to a user who receives a strong signal from an adjacent sector, that neighboring sector is prevented from utilizing the time-frequency bins allocated to this user. This will often occur for terminals located close to the sector side boundaries, where their received signal strength is furthermore weakened by the beam pattern. Therefore, the transmit power is boosted by 3 dB in bins intended for such terminals.[6] The coordination reduces the number of usable bins. We below set this loss to 1/8 of the bins [16], so the spectral efficiency is reduced by a factor $c_1 = 7/8$.

V. THE SPECTRAL EFFICIENCY IN AN INTERFERENCE-LIMITED ENVIRONMENT

The strategies suggested above have been evaluated for a hexagonal cell pattern with 60° sectors, in an interference-limited environment. We take the path loss and short term fading, modelled as Rayleigh fading into account, while the present preliminary investigation does not include shadow fading (log-normal fading).[7] For all details, please see [16].

A. Path Loss and Interference

The path loss is described by a simple power law $r^{-\alpha}$. The average signal-to-interference ratio (SIR) at distance r from the transmitter is assumed given by

$$\bar{\gamma} = \frac{\frac{1}{r^\alpha}P_s(\theta)}{\ell(\sum_i \frac{1}{r_i^\alpha}P_I(\varphi) + I_s(\theta))} \quad . \tag{1}$$

Here, α is the path loss exponent, i is a sum over all interfering sectors, $P_s(\theta)$ is the angle-dependent antenna pattern, ℓ is the traffic load factor in interfering cells, $P_I(\varphi)$ is the transmit power of an interfering antenna at angle φ, r_i is the distance to interferer i, and $I_s(\theta)$ is interference from adjacent sectors of the same site. Noise is neglected in this investigation, so $\bar{\gamma}$ and all results become invariant with respect to the absolute length and power scales.

The strategies introduced in Section IV affect the spectral efficiency in two ways: They reduce the interference at the price of increasing the frequency reuse factor from 1 to $1/(c_1 c_2)$. Assume equal traffic requirement per unit area and the use of the same resource allocations s_1/s and s_2/s in all sectors. The location of the zone border d_1 relative to the total sector side length d then determines the partitioning of s into s_1 and s_2. This parameter can be optimized to maximize the spectral efficiency averaged over the user locations. For $\ell = 1$ and $\alpha = 4$, the use of d_1/d around 0.6-0.7, corresponding to a frequency reuse of 1.5-2, optimizes the average spectral efficiency. For $\ell = 1$ and $\alpha = 4$, this choice provides coverage with at least 5 dB SIR over the whole sector. The average SIR becomes around 16 dB and 16-QAM or higher modulation formats will be used in approximately 1/3 of the area. The distribution of SIR within a 60 degree sector is illustrated by Fig. 4. Note how the SIR is increased stepwise at the zone boundary, since the number of interfering sites is reduced by 2/3 in the outer zone 2 as compared to the inner zone 1.

B. Path Loss, Interference and Rayleigh Fading

Rayleigh fading is now added to the path loss model (1), and MRC with L antennas is assumed in the terminals. The average of the spectral efficiency over the sector area is then evaluated assuming the adaptive OFDM downlink of Section III, with the adaptive modulation rate region boundaries of Table I. The coverage and spectral efficiency will depend crucially on the assumed scheduling strategy. We here assume that the

---

[6]An alternative would be to transmit simultaneously from both sectors, analogous to the "softer handover" concept of WCDMA. This is a worse alternative since the sum of received powers when using simultaneous transmission would in general be less than when the power of the strongest path is doubled while the weaker path is set to zero.

[7]We would not expect that addition of log-normal shadow fading alters the total capacity significantly for delay-insensitive traffic. It would just increase the variability of the SIR encountered by terminals. However, shadow fading has a crucial effect on delay-sensitive traffic. This is a topic of current research.
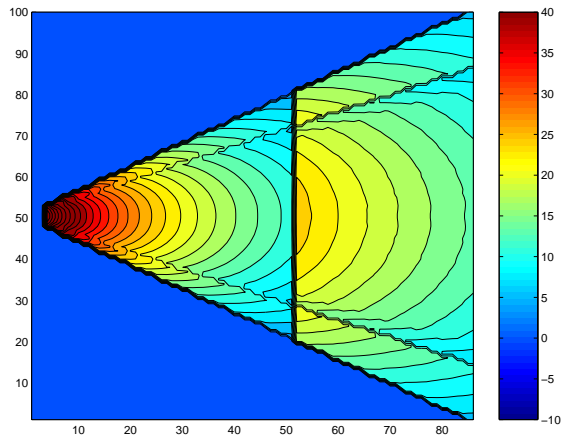
Fig. 4. Distribution of the SIR in dB within a 60 degree sector, with zone boundary $d_1 = 0.60d$. The axes are scaled by $100d$. The traffic load factor is $\ell = 1$ and the propagation exponent is $\alpha = 4$. The inner zone 1 is affected by interference from 36 sites (three tiers), while 12 sites interfere in the outer zone 2.
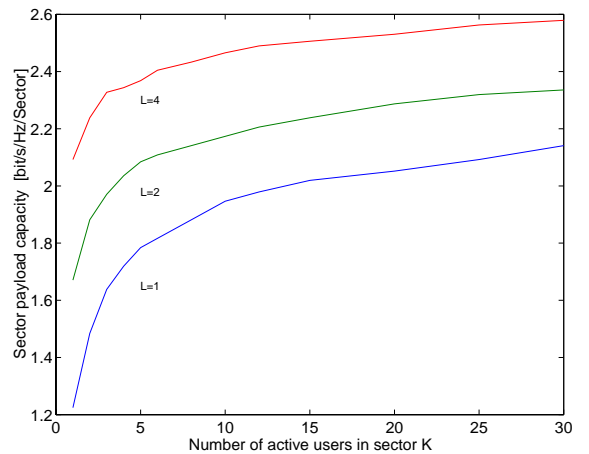

Fig. 5. Estimated sector payload capacity for Rayleigh fading channels in OFDM bins, including all overhead and reuse factors, as a function of the number of active users K, who all have L receiver antennas and use MRC combining. The zone boundary is $d_1 = 0.7d$, the traffic load factor is $\ell = 1$ (full load) and $\alpha = 4$. The equivalent frequency reuse factor is here 1.73.

probability that a user is allocated a bin is made *independent of the absolute average SIR*, and is thus independent of the position within the sector.[8] For Rayleigh fading, a scheduler that selects the terminal with the best SIR *relative* to its own average SIR, measured on a dB scale, maximizes the spectral efficiency under this constraint of position-independent access to time-frequency resources. This scheduler is used below.

For one user per sector, the resulting average spectral efficiency can be evaluated analytically, while Monte-Carlo simulation has been used for $K > 1$ users. This has been done for best effort traffic, assuming constant channels within bins and perfect channel estimation and prediction. K users were distributed randomly within the sector. For each user, the average SIR was calculated by (1) and channels with the corresponding average energy were generated with a Gaussian distribution. After L-branch MRC at the receiver, the scheduler outlined above selected a winner, who was allowed to use the bin. The average over the sector of the throughput within correct link-level packets, $\bar{\eta}_f$ [bit/s/Hz/sector], was estimated. The overhead of our adaptive OFDM system due to 12 pilot/control symbols per bin and the cyclic prefix, results in the *sector payload capacity* $C = 0.811\bar{\eta}_f$ [bit/s/Hz/sector]. Fig. 5 shows results based on 10000 trials. There is a notable improvement with an increasing multiuser selection diversity (increasing K) and of course also an improvement with the number of antennas. The reuse factor $1/(c_1 c_2)$ is here 1.73.

The capacity obtained in Fig. 5 is very similar to the theoretical results obtained in [4], scaled down by the reuse factor 1.73. The assumptions here and in [4] are identical, except that all users were assumed to have the same average SIR of 16 dB in [4], while the users in Fig. 5 have different average SIR, with an overall average close to 16 dB.

---

[8]While all users are thus provided "equal access", their usable data rates will of course depend on their SIRs and positions. This seems reasonable for best-effort traffic, but may be inappropriate for other traffic classes.

REFERENCES

[1] J. Chuang and N. Sollenberger, "Beyond 3G: Wideband wireless data access based on OFDM and dynamic packet assignment," *IEEE Communications Magazine*, July 2000, pp. 78-87.
[2] N. C. Ericsson, S. Falahati, A. Ahlén and A. Svensson, "Hybrid type-II ARQ/AMS supported by channel predictive scheduling in a multi-user scenario," *IEEE VTC2000-Fall*, Boston, MA, USA, Sept. 2000.
[3] Online: www.signal.uu.se/Research/PCCwirelessIP.html.
[4] W. Wang, T. Ottosson, M.Sternad, A. Ahlén and A. Svensson, "Impact of multiuser diversity and channel variability on adaptive OFDM" *VTC 2003-Fall*, Orlando, FL, Oct. 2003.
[5] R.H. Frenkiel, B.R. Badrinath, J. Borras and R.D. Yates, "The Infostation challenge: Balancing cost and ubiquity in delivering wireless data", *IEEE Personal Comm.*, pp. 66-71, April 2000.
[6] S. T. Chung and A. J. Goldsmith, "Degrees of freedom in adaptive modulation: a unified view," *IEEE Trans. Commun.*, Vol. 49, No. 9, pp. 1561-1571, Sept. 2001.
[7] S. Falahati, A. Svensson, M. Sternad and T. Ekman, "Adaptive modulation systems for predicted wireless channels," *IEEE Globecom*, San Fransisco, CA, Dec. 2003.
[8] R. Knopp and P.A. Humblet, "Multiple-accessing over frequency-selective fading channels," *IEEE PIMRC*, pp. 1326-1330. Toronto, Canada, Sept. 27-29 1995.
[9] T. Ottosson, A. Ahlén, A. Brunström, M. Sternad and A. Svensson, "Toward 4G IP-based wireless systems: A proposal for the uplink." *5th and 6th Wireless World Research Forum Meetings*, Tempe, AR, March 2002 and London, June 2002.
[10] T-S Yang and A. Duel-Hallen, "Adaptive modulation using outdated samples of another fading channel" *IEEE WCNC'02*, March 17-21 2002.
[11] M. Sternad and D. Aronsson "Channel estimation and prediction for adaptive OFDM downlinks," *VTC 2003-Fall*, Orlando, FL, Oct. 2003.
[12] S. Falahati, A. Svensson, M. Sternad and H. Mei, "Adaptive trellis-coded modulation over predicted flat fading channels," *VTC 2003-Fall*, Orlando, FL, Oct. 2003.
[13] N. C. Ericsson, *On Scheduling and Adaptive Modulation in Wireless Communications*. Licentiate Thesis, Signals and Systems, Uppsala University, Sweden, June 2001.
[14] T. Ekman, *Prediction of Mobile Radio Channels. Modeling and Design*. PhD Thesis, Signals and Systems, Uppsala University, Sweden, 2002. Online: www.signal.uu.se/Publications/abstracts/a023.html
[15] T. Ekman, M. Sternad and A. Ahlén, "Unbiased power prediction on broadband channels," *IEEE VTC*, Fall 2002, Vancouver, Sept. 2002.
[16] M. Sternad, "Reuse Partitioning and System Capacity in the Adaptive OFDM Downlink of the Wireless IP Project Target System," *Technical Report*, Signals and Systems, Dept, of Engineering Sciences, Uppsala Univ., July 2003. www.signal.uu.se/Publications/abstracts/r0301.html